A FIELD TEST FOR THE MIXED-MODE FRACTURE TOUGHNESS OF WEAK LAYERS

Valentin Adam[1,2,*], Bastian Bergfeld[2], Florian Rheinschmidt[1], Melin D. E. Walet[2], Jakob Schöttner[2], Philipp Weißgraeber[3], Alec van Herwijnen[2], Philipp L. Rosendahl[1]

[1] *Technical University of Darmstadt, Institute of Structural Mechanics and Design, Darmstadt, Germany*
[2] *WSL Institute for Snow and Avalanche Research SLF, Davos Dorf, Switzerland*
[3] *University of Rostock, Chair of Lighweight Design, Rostock, Germany*

ABSTRACT: The triggering mechanisms of dry snow slab avalanches are subjected to a mixed-mode loading scenario driven by different dynamic loading conditions and the natural inclined terrain. However, standard propagation saw tests, which are common to determine the fracture toughness of weak layers, almost exclusively cover the slope-normal regime (mode I) of the anticrack phenomena within these layers. By employing a mechanical model, we introduce a novel conclusive experimental setup that effectively addresses the thus far unexplored shear-influence regime (mode II).

Keywords: Dry-snow slab avalanches, fracture toughness, anticrack propagation, mixed-mode loading, weak snow layers.

1. INTRODUCTION

The description of material failure requires a conclusive criterion that considers parameters relevant to the specific nature of the failure. While there is agreement on the basic physics of fracture within weak snowpack layers, there is no sufficient basis in material properties to quantify it accurately (Rosendahl and Weißgraeber, 2020b). In the last two decades, we have witnessed a paradigm shift describing weak-layer failure as mixed-mode anticracks rather than pure shear (Heierli and Zaiser, 2008). While strength-based bulk-material failure properties have been identified under mixed loading conditions (normal and in-plane shear, Reiweger et al., 2015), energy-based fracture properties under mixed-mode conditions are largely missing.

An established method to derive the fracture toughness of weak layers is the propagation saw test (PST), which has gained widespread recognition since winter season 2005/06 (van Herwijnen and Jamieson, 2005; Gauthier and Jamieson, 2006; Sigrist, 2006). However, due to its geometry and the way it is performed, the critical energy release rate (ERR) has mostly been determined in pure or close-to-pure mode I conditions. Recently Bergfeld et al. (2023a) measured ratios of mode II contributions less than 10% in flat field PST experiments. Nevertheless, significantly more mode II contributions have never been measured, and nothing is known about the behavior of the ERR in the interaction regime. Clearly, the origin of fracture is not solely driven by the normal component of the slope, but also by the in-plane shear component (mode II), especially when considering inclined terrain and the superposition of dynamic loads caused by mountaineers (Mede et al., 2020; Rosendahl and Weißgraeber, 2020a).

Moreover, there is no agreement whether critical cut lengths a_c in PSTs decrease (Gaume et al., 2017; Trottet et al., 2022), increase (Gauthier and Jamieson, 2008; McClung, 2009), or remain constant with slope inclination φ (Bair et al., 2012). This is directly related to the question of whether the compression or shear fracture toughness is larger, as well as how much energy the PST system can release within the weak layer at different slope inclinations.

We propose a novel approach to measure critical cut length on steep angles and address the entire range of mode interactions between compression and in-plane shear. The method is based on a modified PST setup combined with a closed-form mechanical model.

2. MECHANICAL MODEL

Notched samples represent a standard approach in fracture mechanics for the determination of fracture toughnesses (Rosendahl et al., 2019). An example is the double cantilever beam (DCB) test (Hutchinson and Suo, 1991). Due to the artificially introduced cut, stresses at the crack tip become singular, making the energy release the sole driver of failure. This is the reason why the PST is well-suited for measuring the fracture toughness of the weak layer—namely, the energy released per unit crack advance required for crack growth (Weißgrae-

*Corresponding author address:
Valentin Adam, Institute of Structural Mechanics and Design,
Technical University Darmstadt,
Franziska-Braun-Straße 3, 64287 Darmstadt, Germany;
email: valentin.adam@slf.ch

ber and Rosendahl, 2018).

However, determining this ERR is challenging because PSTs are complex systems characterized by different layerings and material properties. To make accurate assessments of their deformations under various boundary conditions, a well-representative model is necessary. Therefore, we analyzed the experiments using a closed-form and well-validated analytical model (Rosendahl and Weißgraeber, 2023), which represents the slab as a shear-deformable, layered plate under cylindrical bending supported by an elastic foundation (weak layer). It enabled us to consider the natural stratification of the slab and the anisotropy of the weak layer. Moreover, it is computationally efficient, making real-time calculations possible. For the purpose of this study, we have implemented the capability to apply a surface line load. With help of the model we calculated the total ERR, and distinguished its mode I and mode II contributions for various scenarios. It enabled to determine a experimental setup which is capable to address the lack of mode II contributions and can simultaneously serve as interpretation tool for possible outcomes.

3. MIXED-MODE FRACTURE TEST

To explore significant mode II contributions to the total ERR, specific modifications of the standard PST are required. The adaptions include i) a reduced slab height and smaller dimensions allowing to ii) tilt the extracted snow column to high inclinations while iii) cutting in downslope direction with iv) additional dead weight on the slab.

3.1. Experimental setup

The first intuitive measure to increase mode II contributions is to tilt a PST configuration up to naturally not feasible inclinations. Therefore transportable specimen dimensions are needed, as a snowblock within the weak layer has to be mounted on a tiltable device (Fig. 1). Dimensions of $100\,\mathrm{cm}$ length $30\,\mathrm{cm}$ width and a reduced slab height of $12.5\,\mathrm{cm}$ are chosen. The height-to-length ratio $(1/8)$ is appropriately aligned with the beam theory used in the mechanical model, and the width equals that of a standard PST. However, removing a part of the slab also removes its dead weight as the crack driving force and therefore increases critical cut lengths. An additional surface load is included in our case to compensate for the loss of weight. To prevent any impact on the stiffness of the slab, the weights are positioned freely within prepared notches on the surface of the slab. The specified line load of $1.5\,\mathrm{kN/m}$ translates to a total dead weight of $45\,\mathrm{kg}$, which aligns with a plausible estimation for a previous slab thickness of around $55\,\mathrm{cm}$. For the calculations, we

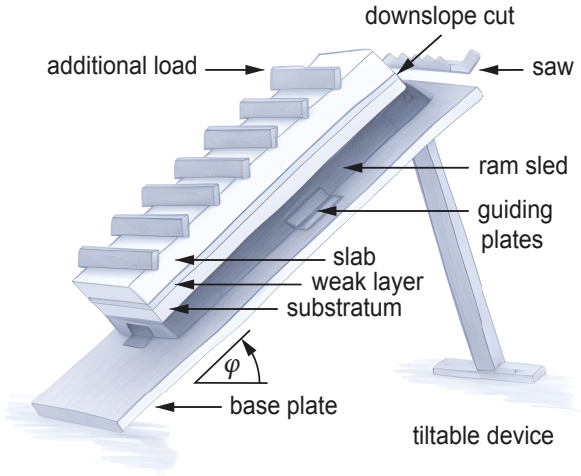

Figure 1: Sketch of a possible setup for the proposed modifications to the standard PST to increase mode II contributions and cover the whole mode interaction regime. Image generated with help of Vizcom (2023).

assume a homogeneous slab with rounded grains (hardness: P), as layering effects are minimized due to the reduced slab height. The respective density of $270\,\mathrm{kg/m^3}$ (Geldsetzer and Jamieson, 2000) is then transformed into elastic properties using the density-parametrization method (Gerling et al., 2017)

$$E_{\mathrm{sl}}(\rho) = E_0 \left(\frac{\rho}{\rho_0}\right)^{4.4}, \tag{1}$$

where $E_0 = 6.5 \cdot 10^3$ MPa (Bergfeld et al., 2023b) and $\rho_0 = 917\,\mathrm{kg/m^3}$ are Young's modulus and density of ice (Northwood, 1947; Mellor and Cole, 1983; Moslet, 2007). We attributed an assumed Young's modulus of $0.2\,\mathrm{MPa}$ and a shear modulus of $0.08\,\mathrm{MPa}$ to the elastic property of the weak layer, corresponding to a Poisson's ratio of $\nu = 0.25$.

3.2. Downslope cuts are mandatory

With the novel setup it is possible to reach a higher mode II fraction (Fig. 2a, solid lines) in comparison to previous performed PSTs (green bullets, van Herwijnen et al. (2016)) by increasing the slope inclination. Despite the gap in our understanding of how the critical cut length qualitatively changes with slope inclination, it is evident that shorter cut lengths lead to a faster increase in mode II interaction. Adding surface line load (Fig. 2a, dashed lines) results in a more pronounced increase of the mode ratio for downslope cuts ($\varphi > 0°$), but in an opposite behaviour for upslope cuts ($\varphi < 0°$). The historical dataset suggests that the amount of mode II measured thus far has been limited to a small fraction

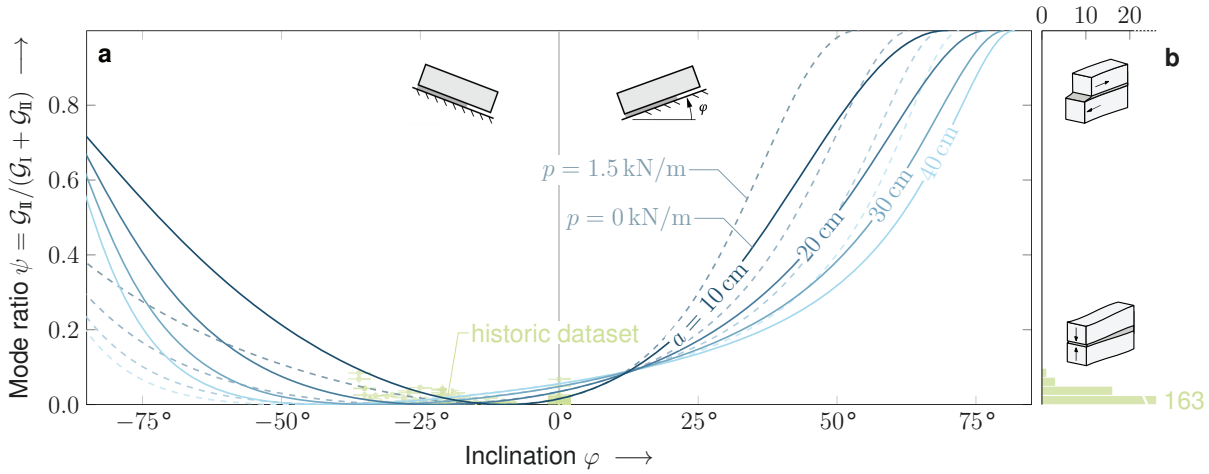

Figure 2: **a** Mode ratio ψ representing the mode II contribution of the ERR at the onset of unstable crack propagation. Calculated for the proposed PST configuration for different cut length in downslope ($\varphi > 0°$) and upslope direction ($\varphi < 0°$). Once with additional lineload ($p = 1.5\,\mathrm{kN/m}$, dashed lines) and without (solid line). The historical dataset collected by van Herwijnen et al. (2016) ($N = 183$, green bullets) consists solely of upslope cuts ($\varphi \leq 0°$) involving several different weak layers and slab assemblies. **a** The number of historical PSTs indicates that no conclusion can be drawn regarding the effect of mode II contributions on the critical ERR with the standard setup.

(Fig. 2b), and even with the new setup, it is not feasible to exceed more than 70 % with upslope cuts (Fig. 2a). On the other hand, downslope cutting leads to a significant increase, with mode ratios approaching pure mode II at slope inclinations around 70° for smaller cut lengths.

The reason for this asymmetrical behavior, with its minimum not at zero but shifted towards the upslope cuts, can be attributed to two effects. The first effect, mentioned already by Sigrist and Schweizer (2007) and recently by Weißgraeber and Rosendahl (2023), is more pronounced in lower inclinations, while the second effect gains importance with steeper inclinations:

1. The natural shear component caused by the dead weight at the crack tip always aligns with the direction of gravitational force. An additional component due to the bending of the slab points in the same direction with downslope cuts and in the opposite direction with upslope cuts.

2. This amplifying and vanishing effect of mode II is further compounded by the influence of bending moments arising from the slab's normal faces. Overhanging (downside face) or missing (upside face) parts lead to an increase of mode I during upslope cutting and to a reduction during downslope cutting.

The novel setup incorporates these aspects with help of the model allowing for shear deformation and capturing rotational inertia of the slab. It becomes evident that, unlike the current standard, downslope cuts are essential to attain nearly pure mode II contributions at feasible inclinations. However, this assumption relies on the condition that the critical cut lengths remain relatively small.

3.3. Need for additional load

The effectiveness of the described setup to cover the whole mode interaction regime is closely linked to the yet unknown response of the critical cut length a_c to increasing slope inclinations. From a practical point of view, the use of very steep angles should be avoided, as it becomes challenging to secure the snowblock onto the tilting device and prevent the additional weights from falling. Conversely, the critical cut length should neither exceed half the PST length to avoid boundary effects, nor decrease to a value close to zero to prevent triggering before higher shear contributions can be reached. To gain a preliminary understanding of the most probable scenario, we adopt a common quadratic energy-based failure criterion for the interaction regime, given by:

$$\left(\frac{\mathcal{G}_\mathrm{I}}{\mathcal{G}_\mathrm{Ic}}\right)^2 + \left(\frac{\mathcal{G}_\mathrm{II}}{\mathcal{G}_\mathrm{IIc}}\right)^2 = 1 \qquad (2)$$

We then investigate the critical cut length in relation to various pure mode ratios $\mathcal{G}_\mathrm{IIc}/\mathcal{G}_\mathrm{Ic}$ (Fig. 3b). A quadratic interaction law is common for materials underlying mixed-mode conditions of shear and tension, while most of them have a larger pure shear fracture toughness than pure tension fracture toughness (Hutchinson and Suo, 1991). The pure compression fracture toughness in this case has been fixed to the median value of the historic dataset

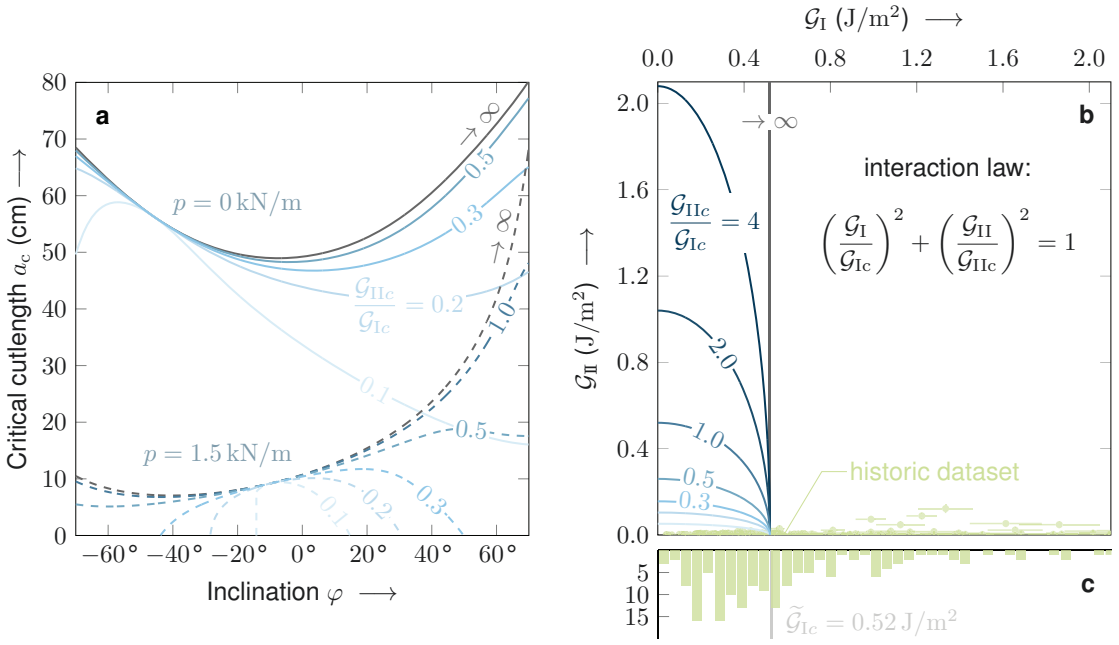

Figure 3: **a** Calculated critical cut length a_c for different ratios of pure mode toughness $\mathcal{G}_{\mathrm{IIc}}/\mathcal{G}_{\mathrm{Ic}}$. With additional surface line load ($p = 1.5\,\mathrm{kN/m}$, dashed lines) and without (solid lines). A quadratic interaction law was assumed to apply an energy based failure criteria as basis of the calculation. **b** Illustration of the interaction law subjected to changes in the ratio of pure mode toughness ($\mathcal{G}_{\mathrm{IIc}}/\mathcal{G}_{\mathrm{Ic}}$). The pure fracture toughness of mode I has been set to the median value of the historical dataset (van Herwijnen et al., 2016), as the experiments are conducted in regimes close-to-pure mode I. The pure mode II fracture toughness $\mathcal{G}_{\mathrm{IIc}}$ varies with the provided ratios, and the interaction behavior between the pure mode toughness values is described quadratic. No conclusions can be made with the historic dataset (green bullets) about the shape of the interaction law. **c** The distribution of historic $\mathcal{G}_{\mathrm{Ic}}$ values and their median $\widetilde{\mathcal{G}}_{\mathrm{Ic}} = 0.52\,\mathrm{J/m^2}$ spanning over a wide range of energy release rates, which can be attributed to the different kinds of investigated weak layers.

$\widetilde{\mathcal{G}}_{\mathrm{Ic}} = 0.52\,\mathrm{J/m^2}$ (Fig. 3c). First and foremost, it can be stated that achieving a practical critical cut length without an additional line load is not feasible with pure critical mode ratios exceeding $\mathcal{G}_{\mathrm{IIc}}/\mathcal{G}_{\mathrm{Ic}} = 0.1$ (depicted by the solid lines in Fig. 3a). An additional line load is necessary to reduce the critical cut length to an applicable size, ensuring the application of the shortened PST length (Fig. 3a, dashed lines).

3.4. Choosing a suitable extra load

If, in the presence of the line load $p = 1.5\,\mathrm{kN/m}$, the pure mode II energy release rate (ERR) is equal to or greater than mode I ($\mathcal{G}_{\mathrm{IIc}}/\mathcal{G}_{\mathrm{Ic}} \geq 1$), the critical cut length increases exponentially for downslope cuts. Values below approximately $\mathcal{G}_{\mathrm{IIc}}/\mathcal{G}_{\mathrm{Ic}} = 0.5$ result in a decreasing trend. In this scenario, the additional line load would not be suitable, as the weak layer could potentially be triggered at lower inclinations. To facilitate the selection of the line load with respect to observed critical cut length, Fig. 4 provides graphical assistance. The plot assists the decision-making which line load is practical to choose to reduce the required inclination for observed trends of critical cut length to reach an amount of 90% mode II. As an example, considering the additional line load of $p = 1.5\,\mathrm{kN/m}$ and a potential critical cut length of 30 cm, the required inclination to achieve a 90% mode II ratio can be decreased by approximately 10°, from 73° to 63°. It is also visible that this effect diminishes with even higher loads. It illustrates that, particularly when dealing with short cut lengths, even a minor increase in the applied additional load can significantly reduce the required angle and thus ensure the feasibility of the experimental procedure.

3.5. Unlocking pure shear is challenging

A possible limitation of the proposed setup could be the domain of high mode II interaction above 80%. Experimentally approaching the point of vanishing mode I, which reveals pure shear behavior, is challenging due to the asymptotic nature of the mode ratio ψ in this regime (Fig. 2a). This requires steeper inclinations, and additionally tension at the crack tip must be prevented. Furthermore, the critical cut length increases with increasing slope inclinations for downslope cuts when the pure mode II

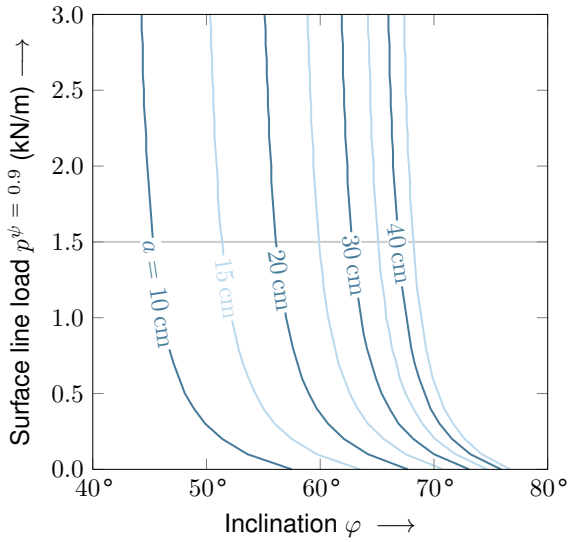

Figure 4: Additional surface lineload $p^{\psi=0.9}$ needed to reach a mode II ratio of $\psi = 90\%$ to the corresponding required inclinations. The plots of the various cut lengths should provide guidance for determining an appropriate additional load for the test setup. The additional surface line load of $p = 1.5\,\mathrm{kN/m}$ used in this study is represented in gray and corresponds to a total dead weight of $45\,\mathrm{kg}$ relative to the provided dimensions.

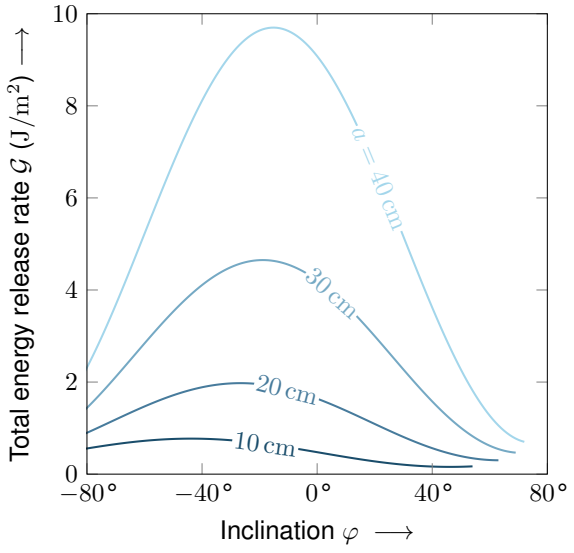

Figure 5: The total ERR $\mathcal{G}$ of the PST configuration, which includes a surface line load of $p = 1.5\,\mathrm{kN/m}$, is calculated for varying slope inclinations and different cut lengths.

fracture toughness is equal to or greater than half of the pure mode I fracture toughness (as depicted in Fig. 3a). The reason for increasing critical cut length even below the 1-to-1 ratio of pure mode toughness can be attributed to the fact that the total ERR of the PST system has its peak at upslope cuts between $-10°$ and $-45°$ depending on the cut length and decreases towards higher inclinations for downslope cuts (Fig. 5). The ability of the slabs to bend and release energy within the weak layer through deformation is more pronounced at lower angles. These circumstances can lead to the requirement of a considerably larger additional load at higher inclinations, which can be challenging to practically achieve. Nonetheless, achieving coverage up to 80% is already a significant improvement, as pure shear is excepted to be rare in real-life scenarios.

4. CONCLUSIONS

In this study, we introduced a novel experimental setup capable of addressing mode II contributions to the critical ERR of weak layers that have not been previously explored. The mechanical model assisted in deriving modifications to the standard PST setup:

1. Steeper slope inclinations reveal the possibility to address the whole range of mode interaction from pure compression (mode I) to pure shear (mode II), whereby a reduced slab height and a beam length of 1 m ensure a good handling of the extracted snow block.
2. Downslope cuts result in a faster increase of mode II energy release rates and are necessary to reach a significant contribution at feasible inclinations.
3. Additional dead weights on the surface of the slab are needed to reduce the critical cut length to an acceptable length.
4. Due to the decrease of the total ERR of the system the probability of increasing cut length with increasing slope inclinations for downslope cuts is high. Therefore close-to-pure mode II contributions might practically be difficult to realise as a substantial additional amount of weight is needed.

ACKNOWLEDGEMENT

This work was in part supported by grants from the Swiss National Science Foundation (200021_169424 and 200021L_201071) and funded by the Deutsche Forschungsgemeinschaft (DFG, German Research Foundation) under grant no. 460195514.

We used `https://chat.openai.com` and `https://www.deepl.com/write` to improve ease of reading and comprehension.

CODE AVAILABILITY

A Python implementation of the mechanical model is available from the code repository `https://github.com/2phi/weac` or for direct installation from `https://pypi.org/project/weac` (last accessed July 24, 2023).

References

Bair, E. H., Simenhois, R., Birkeland, K., and Dozier, J. (2012). A field study on failure of storm snow slab avalanches. *Cold Regions Science and Technology*, 79-80:20–28.

Bergfeld, B., van Herwijnen, A., Bobillier, G., Rosendahl, P. L., Weißgraeber, P., Adam, V., Dual, J., and Schweizer, J. (2023a). Temporal evolution of crack propagation characteristics in a weak snowpack layer: conditions of crack arrest and sustained propagation. *Natural Hazards and Earth System Sciences*, 23(1):293–315.

Bergfeld, B., van Herwijnen, A., and Schweizer, J. (2023b). Time series data on dynamic crack propagation in long propagation saw tests. *EnviDat*.

Gaume, J., van Herwijnen, A., Chambon, G., Wever, N., and Schweizer, J. (2017). Snow fracture in relation to slab avalanche release: critical state for the onset of crack propagation. *The Cryosphere*, 11(1):217–228.

Gauthier, D. and Jamieson, B. (2006). Understanding the Propagation of Fractures and Failures Leading to Dangerous and Destructive Snow Avalanches: Recent Developments. *Annual Conference of the Canadian Society for Civil Engineering, First Specialty Conference on Disaster Mitigation*, pages 1–9.

Gauthier, D. and Jamieson, B. (2008). Evaluation of a prototype field test for fracture and failure propagation propensity in weak snowpack layers. *Cold Regions Science and Technology*, 51(2-3):87–97.

Geldsetzer, T. and Jamieson, B. (2000). Estimating dry snow density from grain form and hand hardness. In *International Snow Science Workshop*, pages 121–127.

Gerling, B., Löwe, H., and van Herwijnen, A. (2017). Measuring the Elastic Modulus of Snow. *Geophysical Research Letters*, 44:11,088–11,096.

Heierli, J. and Zaiser, M. (2008). Failure initiation in snow stratifications containing weak layers: Nucleation of whumpfs and slab avalanches. *Cold Regions Science and Technology*, 52(3):385–400.

Hutchinson, J. W. and Suo, Z. (1991). Mixed Mode Cracking in Layered Materials. In *Journal of Applied Mechanics*, volume 27, pages 63–191.

McClung, D. M. (2009). Dry snow slab quasi-brittle fracture initiation and verification from field tests. *Journal of Geophysical Research*, 114(F1):F01022.

Mede, T., Chambon, G., Nicot, F., and Hagenmuller, P. (2020). Micromechanical investigation of snow failure under mixed-mode loading. *International Journal of Solids and Structures*, 199:95–108.

Mellor, M. and Cole, D. M. (1983). Stress/strain/time relations for ice under uniaxial compression. *Cold Regions Science and Technology*, 6(3):207–230.

Moslet, P. (2007). Field testing of uniaxial compression strength of columnar sea ice. *Cold Regions Science and Technology*, 48(1):1–14.

Northwood, T. D. (1947). Sonic determination of the elastic properties of ice. *Canadian Journal of Research*, 25a(2):88–95.

Reiweger, I., Gaume, J., and Schweizer, J. (2015). A new mixed-mode failure criterion for weak snowpack layers. *Geophysical Research Letters*, 42(5):1427–1432.

Rosendahl, P. L., Staudt, Y., Odenbreit, C., Schneider, J., and Becker, W. (2019). Measuring mode I fracture properties of thick-layered structural silicone sealants. *International Journal of Adhesion and Adhesives*, 91:64–71.

Rosendahl, P. L. and Weißgraeber, P. (2020a). Modeling snow slab avalanches caused by weak-layer failure – Part 1: Slabs on compliant and collapsible weak layers. *The Cryosphere*, 14(1):115–130.

Rosendahl, P. L. and Weißgraeber, P. (2020b). Modeling snow slab avalanches caused by weak-layer failure – Part 2: Coupled mixed-mode criterion for skier-triggered anticracks. *The Cryosphere*, 14(1):131–145.

Rosendahl, P. L. and Weißgraeber, P. (2023). Weak Layer Anticrack Nucleation Model.

Sigrist, C. (2006). Measurement of fracture mechanical properties of snow and application to dry snow slab avalanche release. *PhD Thesis*, (16736):1–158.

Sigrist, C. and Schweizer, J. (2007). Critical energy release rates of weak snowpack layers determined in field experiments. *Geophysical Research Letters*, 34(3).

Trottet, B., Simenhois, R., Bobillier, G., Bergfeld, B., van Herwijnen, A., Jiang, C., and Gaume, J. (2022). Transition from subrayleigh anticrack to supershear crack propagation in snow avalanches. *Nature Physics*, 18:1–5.

van Herwijnen, A., Gaume, J., Bair, E. H., Reuter, B., Birkeland, K. W., and Schweizer, J. (2016). Estimating the effective elastic modulus and specific fracture energy of snowpack layers from field experiments. *Journal of Glaciology*, 62(236):997–1007.

van Herwijnen, A. and Jamieson, B. (2005). High-speed photography of fractures in weak snowpack layers. *Cold Regions Science and Technology*, 43(1-2):71–82.

Vizcom (2023). Image generated by ai assistant. Online generation. Generated by Vizcom.

Weißgraeber, P. and Rosendahl, P. L. (2018). Schneebrettlawinen. Bruchmechanik der Schwachschicht. *Bergundsteigen #105*, 27(4):70–77.

Weißgraeber, P. and Rosendahl, P. L. (2023). A closed-form model for layered snow slabs. *The Cryosphere*, 17(4):1475–1496.